A 20-Mb/s VLC Link With a Polymer LED and a Multilayer Perceptron Equalizer

Haigh, P. A. , Bausi, F. , Kanesan, T. , Le, S. T. , Rajbhandari, S. , Ghassemlooy, Z. , Papakonstantinou, I. , Popoola, W. , Burton, A. , Le Min, H. , Ellis, A. D. and Cacialli, F.

Original citation & hyperlink:
Haigh, P. A. , Bausi, F. , Kanesan, T. , Le, S. T. , Rajbhandari, S. , Ghassemlooy, Z. , Papakonstantinou, I. , Popoola, W. , Burton, A. , Le Min, H. , Ellis, A. D. and Cacialli, F. (2014) A 20-Mb/s VLC Link With a Polymer LED and a Multilayer Perceptron Equalizer. IEEE Photonics Technology Letters, volume 26 (19): 1975 – 1978
http://dx.doi.org/10.1109/LPT.2014.2343692

ISSN 1041-1135
DOI 10.1109/LPT.2014.2343692

A 20 Mb/s VLC Link with a Polymer LED and a Multi-Layer Perceptron Equalizer

P. A. Haigh, F. Bausi, T. Kanesan, S. T. Le, S. Rajbhandari, Z. Ghassemlooy, I. Papakonstantinou, W. Popoola, A. Burton, H. Le Minh, A. D. Ellis and F. Cacialli

***Abstract*—This paper experimentally demonstrates a visible light communication system using a 350 kHz polymer light-emitting diode operating at a total bit rate of 19 Mb/s with a bit error rate (BER) of 10^{-6} and 20 Mb/s at the forward error correction limit for the first time. This represents a remarkable net data rate gain of ~ 55 times. The modulation format adopted is on-off keying in conjunction with an artificial neural network classifier implemented as an equalizer. The number of neurons used in the experiment is varied from the set *N* = {5, 10, 20, 30, 40} with 40 neurons offering the best performance at 19 Mb/s and the BER of 10^{-6}.**

***Index Terms*—Artificial neural network, bit error rate, equalizers, organic light emitting diodes, visible light communications**

I. Introduction

Visible light communications (VLC) – the transmission of information over visible wavelengths has become the subject of widespread attention in recent years. The most widely used light sources in VLC are phosphor-converted gallium nitride based white light-emitting diodes (LEDs) [1]. However, in recent years we have started to see development of a new wave of LEDs using organic materials such as polymers. Polymer LEDs (PLEDs) offer a number of advantageous including being eco-friendliness, colour **tunability**, potentially ultra-low costs as materials are deposited by simple room temperature solution based processing methods and the ability to produce large area panels [2]. Research into PLED-based optical communications was first outlined in [3], following which there was no further research activity for a few years. The first practical demonstration of polymer VLC (PVLC) at a transmission speed of 550 kb/s was reported in [4].

The key challenge in conventional VLC of highly bandwidth limited optoelectronic components is heightened in PVLC due to the lower charge mobility statistics in polymer semiconductors. The bandwidth is therefore lower by several orders of magnitude compared to inorganic devices, thus resulting in a substantial challenge when operating at higher data rates. Subsequently research has been focused on increasing the data rate using digital signal processing techniques to overcome the physical device limitations. In [5] the state-of-the-art rate is 10 Mb/s from a 270 kHz bandwidth PLED using a least mean squares (LMS) equalizer in real time with a field programmable gate array (FPGA). In this work we report a doubling of the data rate from 10 Mb/s to 20 Mb/s by adopting the multilayer perceptron (MLP) artificial neural network (ANN) classifier as the equalizer due to its superior mean square error (MSE) convergence and bit error rate (BER) performance [6]. Additionally, the PLED bandwidth used here is extended to ~350 kHz due to thermal annealing during the production; i.e. increasing the active layer crystallinity and therefore charge mobility [7]. Throughout the paper we refer to [5] and make comparisons with the link used in this work in terms of the optoelectronic and BER performance. It should be noted that the signal processing for equalization adopted in [5] and this work is slightly dissimilar; the LMS filter used in [5] was implemented on an FPGA, whereas the ANN used here is implemented offline in MATLAB.

II. Polymer Light Emitting Diode Processing

Polymer semiconductors undergo severe degradation when exposed to oxygen and water molecules in air. Generally these processes are due to oxidation reactions or formation of molecular complexes. They introduce defects in the polymer which can act as charge carrier traps [8]. Hence, air exposure reduces the device lifespan and performance. Thus, to prevent degradation, our devices are encapsulated in a nitrogen atmosphere and no performance degradation was detected.

Manuscript received XX February, 2014.

P. A. Haigh, Z. Ghassemlooy, A. Burton and H. Le Minh are with the Optical Communications Research Group, Northumbria University, Newcastle-upon-Tyne NE1 8ST, UK.

F. Bausi and F. Cacialli are with the Department of Physics and Astronomy, and the London Centre for Nanotechnology, University College London, WC1E 6BT, UK

T. Kanesan is from Telekom Research & Development (TM R&D), TM Innovation Centre, 63000 Cyberjaya, Selangor, Malaysia. S. Le Thai and A. D. Ellis are from the Aston Institute of Photonic Technologies, Aston University, Birmingham, B4 7ET, UK.

S. Rajbhandari is from the Department of Engineering Science, University of Oxford, Parks Road, Oxford OX1 3PJ, UK.

P. A. Haigh and I. Papakonstantinou is with the Department of Electronic and Electrical Engineering, University College London, London, WC1E 7JE, UK.

W. Popoola is with the School of Engineering and Built Environment, Glasgow Caledonian University, Glasgow, G4 0BA, UK.

e-mail: {paul.haigh; z.ghassemlooy}@northumbria.ac.uk; {f.bausi; p.haigh; i.papakonstantinou; f.cacialli}@ucl.ac.uk; {let1; andrew.ellis}@aston.ac.uk wasiu.popoola@gcu.ac.uk.

Glass substrates were used for encapsulation (Ossila Ltd) with a pre-patterned thin layer (~120 nm) of indum tin oxide (ITO) as a transparent anode (Fig. 1). The ITO surface was cleaned by sonication in acetone and isopropanol. An oxygen plasma treatment of the cleaned ITO substrates was done to increase the work function and to reduce the surface roughness [9, 10]. A hole-injection layer (~40 nm) of PEDOT:PSS (Heraeus Clevios™ P VP AI 4083) was deposited via spin-coating (5000 rpm for 30 s in air) on top of the ITO a few seconds after the oxygen plasma. To remove any residue of water from the PEDOT:PSS layer, we annealed the samples at 180°C for 10 minutes in nitrogen atmosphere. The emissive layer of poly[2-methoxy-5-(3′,7′-dimethyloctyloxy)-1,4-phenylenevinylene] (MDMO-PPV) with a M_n of ~23 kg/mol (Sigma-Aldrich) was deposited via spin coating (2,000 rpm for 60 s) from 1% w/w (8.76 g/mL) solution in toluene.

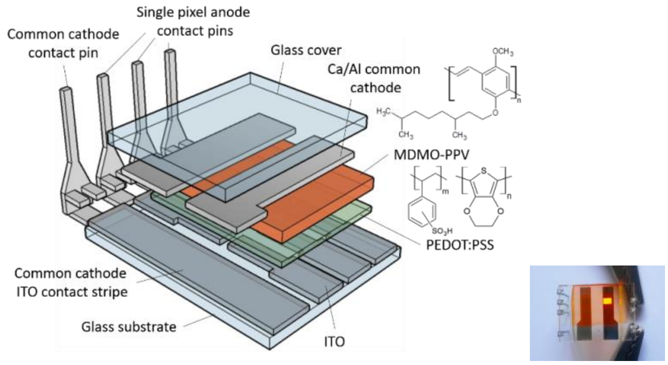

Fig. 1 An exploded schematic of an encapsulated device as described in the text. Inset is a top view photograph of a single photoactive area PLED (3.5 mm^2) driven at 8 V_{DC}

The samples were annealed for 10 minutes above the glass transition temperature, at 150 °C under nitrogen atmosphere. This treatment of the active layer is expected to increase the inter-molecular interaction through the reorganization of the polymer chains. This improves the charge transport [12, 13] resulting in a higher bandwidth of the device compared to the previous work [5]. **As expected, it also causes a partial but acceptable decrease in the luminance from ~5 kcd/m^2 to ~3.5 kcd/m^2 at 10 mA operation (Fig. 2).**

On top of the emissive layer we evaporated 30 nm of metallic calcium as a cathode, covered by 150 nm of a protective layer of aluminum. The devices were encapsulated with a second glass sheet held together by a thin film of epoxy glue (Ossila Ltd). The glue is hardened under UV light for 15 minutes to seal the device. Contact legs were then applied to the finished devices. The L-I-V relationships were measured between 0 – 10 mA (Fig. 2 - solid lines) and compared to non-encapsulated devices (dashed lines) from our previous work [5]. To prevent the metallic cathode from air exposure, it is connected to the pin through a large ITO stripe across the whole device as shown in Fig. 1. This ITO contact introduces a ~ 100 Ω series resistance. The additional resistance can account for the lower current measured at any voltages in the encapsulated device compared to the previous one [5]. A low-pass filter is formed by the series resistance of the diode and the electrodes capacitance and a higher series resistance is expected to lower the cut-off frequency of the filter. However, as reported above, we measured a higher bandwidth for the encapsulated devices than previously [5], probably because the device degradation is prevented. An even higher bandwidth is probably reachable through a better design of the device trying to reduce the resistance in series to the diode.

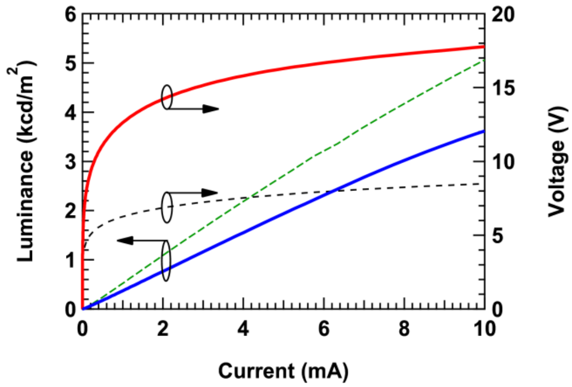

Fig. 2 L-I-V curves of the PLED under test; shown in dashed lines are the diodes used in [5]

III. Test Setup and Artificial Neural Network

The block diagram of the system under test is illustrated in Fig. 3.

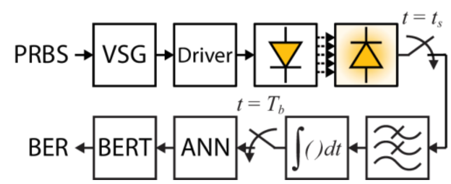

Fig. 3 Schematic block diagram for the system under test

An unbiased 1 V_{AC} peak-to-peak rectangular 2^{15}-1 pseudorandom binary sequence (PRBS) is generated by a Rohde and Schwarz SMBV100A vector signal generator (VSG) at a pre-determined data rate. In [5] the PLED was sub-optimally driven as a voltage sink directly from the VSG. In this work the signal is first amplified then fed into a current converting driver to intensity modulate the PLED while biasing the device in the linear operating region (8 mA DC bias, 6 mA AC). The modulated light is transmitted over the channel, which is represented by a DC gain < 1 [11]. The link distance is 0.05 m, which is very short in comparison to a full room scale. **It should be noted that the experiment was performed using a single 3.5 mm^2 photoactive area pixel, see inset in Fig. 1 and hence the transmission distance could be improved using additional pixels.** Further, the devices were encapsulated allowing transmission outside of a pumped vacuum environment for the first time. The receiver is identical to the one used in [5] thus is not described here. The received signal is sampled and digitized by a Tektronix MDO4104B-6 oscilloscope (1 GHz bandwidth). 10^7 samples per acquisition were recorded with a sampling frequency that was varied according to the data rate to give a maximum of 10 Sa/sym. The data is then loaded in MATLAB for further processing and down-sampled using an integrate and dump method.

Band-limitation leads to inter-symbol interference (ISI), which is well covered in the literature and not repeated here [12]. It is well known that equalization can be used to remove (or considerably reduce) ISI. Employing an ANN classifier as an equalizer is an increasingly popular option in optical wireless communications due to lower MSE performance compared to conventional equalizers [6]. The MLP is the best performing ANN, offering a signal-to-noise ratio (SNR) gain of > 5 dB compared to other classifiers and conventional equalizers [13] and hence is adopted here. The theory of MLP operation can be referred to in literature in an effort to save space [6]. The functional units of the ANN are neurons and in this paper the number of neurons in the hidden layer is varied from the set $N = \{5, 10, 20, 30, 40\}$, which is selected to represent an increasing equalization ability at the cost of increased complexity. In order for the neurons to map the input-output relationship and decision boundary, they must be trained with the Levenberg-Marquardt back propagation algorithm (refer to [6] for the theory and other training algorithms) due to fast convergence and superior MSE performance. In this work the training sequence is varied, with $T_{len} = \{10^3, 10^4, 2^{14}, 2^{15}\}$, which were selected because an increasing training length will provide a better representation of the input-output map and subsequently increase the symbol estimation performance. The maximum training length is equal to the same number of bits ($2^{15} – 1$) in PRBS-15.

IV. Results

The results are analyzed starting with the unequalized case, followed by the equalized performance in descending order of T_{len}. The BER floor is set to 10^{-6} as in [5]. The unequalized BER performance of the link is illustrated in Fig. 4 (a), where transmission speeds up to 2 Mb/s can be supported. This represents a decrease in performance compared to [5] by 1 Mb/s. The reason for the unexpected decrease in performance can be attributed to the PRBS length; which was increased from 2^{10} [5] to 2^{15}. This increase caused an additional ~ 4 dB SNR requirement due to the baseline wander penalty. In Fig. 4 (b) and (c) the eye diagrams for the PLED under test are shown for 1 Mb/s and 2 Mb/s, respectively.

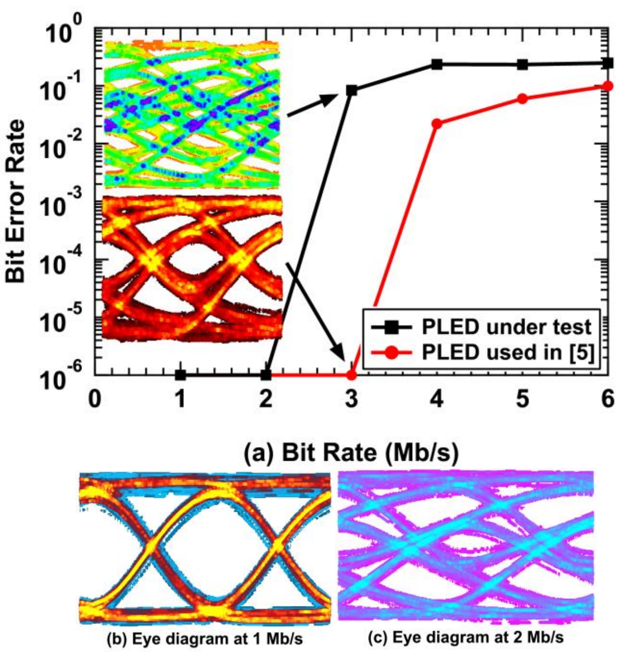

Fig. 4 (a) the raw BER performance in comparison with [5]; a deterioration of 1 Mb/s is noted due to the longer PRBS sequence used. Eye diagrams at 3 Mb/s are shown inset and at (b) 1 Mb/s and (c) 2 Mb/s

The equalized BER performance for $T_{len} = 2^{15}$ is shown in Fig. 5. Setting $N = \{5, 10\}$ can provide an increased data rate up to 8 Mb/s, offering an increase of 6 Mb/s over the unequalized rate. It should be noted that achieving 8 Mb/s at a BER of 10^{-6} represents an increase over the maximum error free data rate reported in [5] by 1 Mb/s. This can be improved by considering the forward error correction (FEC) BER limits of 2×10^{-2} (20 % overhead) and 3.8×10^{-3} (7% overhead) [14]. For $N = 5$; 10 Mb/s can be recovered within the 7% FEC limit, offering a gross data rate of 9.3 Mb/s, equal to [5].

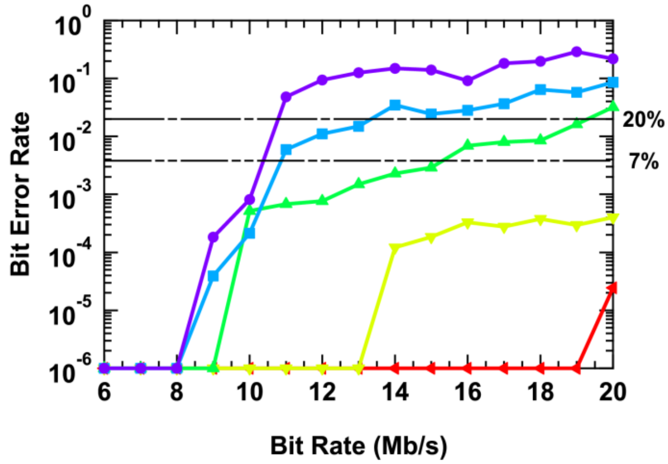

Fig. 5 Equalized BER performance of the link with a training length of 2^{15} and varying number of neurons

Setting $N = 20$ can provide 9 Mb/s, offering an additional 1 Mb/s error free link performance over $N = \{5, 10\}$, however at the 7% FEC limit, a line rate of 15 Mb/s can be achieved, giving a useable data rate of 13.95 Mb/s. At the 20% FEC limit, a line rate of 19 Mb/s can be recovered, resulting in a net data rate of 15.2 Mb/s. In order to achieve error free data rates > 10 Mb/s, it is necessary to increase the number of ANN inputs and neurons to $N = \{30, 40\}$, which can provide 12 and 19 Mb/s at a BER of 10^{-6}, respectively. A data rate of 20 Mb/s can be achieved at a BER of 4×10^{-4} and 2.5×10^{-5} for $N = 30$ and 40, respectively. If $N > 40$, there is no increase in transmission speed available and as such $N = 50$ was not included in the results.

Fig. 6 illustrates the ANN BER performance for $T_{len} = 2^{14}$ and $T_{len} = 10^4$, respectively over the range of neurons. There are few major differences between the two training sequences shown in Fig. 6 (and Fig. 5). The most important difference is that the maximum error free data rate achievable is reduced by 1 Mb/s to 18 Mb/s for $T_{len} = 10^4$. Clearly due to the lack of differences in the equalized BER results, the equalized BER performance effectively becomes independent of the training length when a sufficient input-output map and decision boundary is formed. For $N = \{5, 10\}$ an error free data rate of 8 Mb/s is possible while for $N = 20$, this is increased to 9 Mb/s. For higher orders of N there are slight differences in the achievable transmission speeds where the longer training lengths can offer up to 1 Mb/s advantage over the shorter lengths. As for $N = 30$, error free data rates of 12 Mb/s and 13 Mb/s can be obtained for $T_{len} = 2^{14}$ and $T_{len} = 2^{15}$, respectively. Similarly for $N = 40$, 18 and 19 Mb/s can be attained for $T_{len} = 10^4$ and $T_{len} = 2^{15}$, respectively at a BER of 10^{-6}. Therefore it is possible to infer that the ISI spans 30 to 40 symbols at high data rates. It should be noted that for $N = 50$ there is no improvement at any training length and for data rates > 19 Mb/s, the system becomes noise limited as there is no further improvement by increasing N.

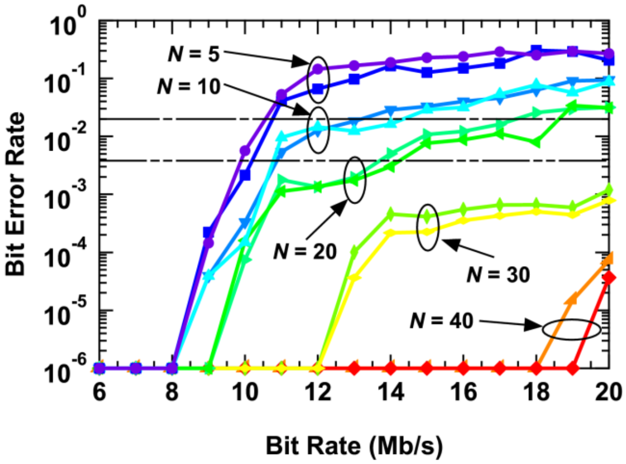

Fig. 6 ANN BER performance of the link with $T_{len} = 2^{14}$ and $T_{len} = 10^4$; offering performance up to 19 and 18 Mb/s, respectively

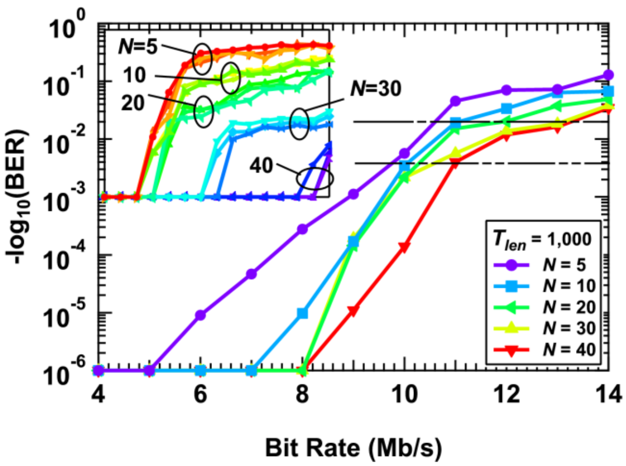

Fig. 7 Equalized BER performance with a training length of 10^3 and varying N; the inset has the same axis range, conclusively illustrating that there are few differences between the equalized results for $T_{len} = \{10^4, 2^{14}, 2^{15}\}$

Finally in Fig. 7 the equalized BER results for $T_{len} = 10^3$ are outlined. A significant reduction in performance can be seen for $N = 5$, as the recoverable error free data rate available is 5 Mb/s; representing a significant reduction in achievable speeds compared to the results for longer training sequences. Considering 7% and 20% FEC limits, line rates of 9 Mb/s and 10 Mb/s can be achieved, respectively. For higher values of N the improvement in data rate is not substantial; 8 Mb/s is the maximum error free rate for $N = \{20, 30, 40\}$ neurons.

It is possible to deduce from the performance degradation that for training lengths < 10^4 the input-output map is not properly formed and the ANN is unable to generalize properly and classify unknown transitions. These results are significant because for the first time, to the best of our knowledge, an error free data rate of slightly lower than 20 Mb/s has been achieved. This represents a 2.7 fold increase over the previously reported state-of-the-art (7 Mb/s) error free data rate and 1.9 fold increase over the highest data rate at 7% FEC reported in [5].

V. Conclusion

We have reported a 20 Mb/s PLED-VLC system for the first time, offering a remarkable improvement of ~10 Mb/s over the previously reported state-of-the-art transmission speed. We have outlined the key differences and improvements throughout. In order to achieve 20 Mb/s a superior ANN equalizer was required at the cost of computational complexity.

Acknowledgments

P. A. Haigh received the full PhD scholarship from Northumbria University. This work is supported by the EU COST Action IC 1101 and the EU FP7 Marie Curie ITN GENIUS - grant number PITN-CT-2010-264694.

References

[1] J. Armstrong, R. J. Green, and M. D. Higgins, "Comparison of Three Receiver Designs for Optical Wireless Communications using White LEDs," *Communications Letters, IEEE,* vol. 16, pp. 748-751, 2012.

[2] H. Klauk, *Organic Electronics: Materials, Manufacturing, and Applications*: Wiley, 2006.

[3] J. Clark and G. Lanzani, "Organic photonics for communications," *Nat Photon,* vol. 4, pp. 438-446, 2010.

[4] P. A. Haigh, Z. Ghassemlooy, H. L. Minh, S. Rajbhandari, F. Arca, S. F. Tedde, O. Hayden, and I. Papakonstantinou, "Exploiting Equalization Techniques for Improving Data Rates in Organic Optoelectronic Devices for Visible Light Communications," *Journal of Lightwave Technology,* vol. 30, pp. 3081-3088, Oct 1 2012.

[5] P. A. Haigh, F. Bausi, Z. Ghassemlooy , I. Papakonstantinou, H. Le Minh, C. Flechon, and F. Cacialli, "Visible Light Communications: Real Time 10 Mb/s Link with a Low Bandwidth Polymer Light-Emitting Diode," *Optics Express,* vol. [In Press], 2014.

[6] S. Haykin, *Neural networks: A comprehensive foundation,* 2nd ed. New Jersey, USA: Prentice Hall, 1998.

[7] T.-Q. Nguyen, R. C. Kwong, M. E. Thompson, and B. J. Schwartz, "Improving the performance of conjugated polymer-based devices by control of interchain interactions and polymer film morphology," *Applied Physics Letters,* vol. 76, pp. 2454-2456, 2000/04/24/ 2000.

[8] H. T. Nicolai, M. Kuik, G. A. Wetzelaer, B. de Boer, C. Campbell, C. Risko, J. L. Bredas, and P. W. Blom, "Unification of trap-limited electron transport in semiconducting polymers," *Nat Mater,* vol. 11, pp. 882-7, Oct 2012.

[9] T. M. Brown and F. Cacialli, "Contact optimization in polymer light-emitting diodes," *Journal of Polymer Science Part B: Polymer Physics,* vol. 41, pp. 2649-2664, 2003 2003.

[10] N. Johansson, F. Cacialli, K. Z. Xing, G. Beamson, D. T. Clark, R. H. Friend, and W. R. Salaneck, "A study of the ITO-on-PPV interface using photoelectron spectroscopy," *Synthetic Metals,* vol. 92, pp. 207-211, 1998.

[11] J. M. Kahn and J. R. Barry, "Wireless infrared communications," *Proceedings of the IEEE,* vol. 85, pp. 265-298, 1997.

[12] S. U. H. Qureshi, "Adaptive equalization," *Proceedings of the IEEE,* vol. 73, pp. 1349-1387, 1985.

[13] S. Rajbhandari, J. Faith, Z. Ghassemlooy, and M. Angelova, "Comparative study of classifiers to mitigate intersymbol interference

in diffuse indoor optical wireless communication links," *Optik - International Journal for Light and Electron Optics,* 2013.

[14] J. G. Proakis, *Digital Communications*. New York: McGraw-Hill, 2004.